

PAPER • OPEN ACCESS

3D printing X-Ray Quality Control Phantoms. A Low Contrast Paradigm

To cite this article: I. Kapetanakis *et al* 2017 *J. Phys.: Conf. Ser.* **931** 012026

View the [article online](#) for updates and enhancements.

You may also like

- [ALMA Deep Field in SSA22: Source Catalog and Number Counts](#)
Hideki Umehata, Yoichi Tamura, Kotaro Kohno et al.
- [Thermal stability studies of plasma sprayed yttrium oxide coatings deposited on pure tantalum substrate](#)
Nagaraj A, Anupama P, Jaya Mukherjee et al.
- [The Effects of Different Gaps on the Weld Morphology, Microstructure and Residual Stress of AH36 Steel were Studied by Laser Arc Hybrid Welding](#)
Xiaoqi Hou, Xin Ye, Xiaoyan Qian et al.



ECS
The
Electrochemical
Society
Advancing solid state &
electrochemical science & technology

DISCOVER
how sustainability
intersects with
electrochemistry & solid
state science research

3D printing X-Ray Quality Control Phantoms. A Low Contrast Paradigm

I. Kapetanakis, G. Fountos, C. Michail, I. Valais, N. Kalyvas*

Department of Biomedical Engineering, Technological Educational Institute of Athens, Egaleo, 122 10 Athens, Greece

e-mail: nkalyvas@teiath.gr

Abstract. Current 3D printing technology products may be usable in various biomedical applications. Such an application is the creation of X-ray quality control phantoms. In this work a self-assembled 3D printer (geetech i3) was used for the design of a simple low contrast phantom. The printing material was Polylactic Acid (PLA) (100% printing density). Low contrast scheme was achieved by creating air-holes with different diameters and thicknesses, ranging from 1mm to 9mm. The phantom was irradiated at a Philips Diagnost 93 fluoroscopic installation at 40kV-70kV with the semi-automatic mode. The images were recorded with an Agfa cr30-x CR system and assessed with ImageJ software. The best contrast value observed was approximately 33%. In low contrast detectability check it was found that the 1mm diameter hole was always visible, for thickness larger or equal to 4mm. A reason for not being able to distinguish 1mm in smaller thicknesses might be the presence of printing patterns on the final image, which increased the structure noise. In conclusion the construction of a contrast resolution phantom with a 3D printer is feasible. The quality of the final product depends upon the printer accuracy and the material characteristics.

Keywords: 3D printing; X-ray; Quality Control;

1. Introduction

Image quality metrics are widely used in the assessment of medical image characteristics. These performance indicators may be objective as well as subjective [1, 2]. The former utilises the concept of Detective Quantum Efficiency (DQE) for calculating the square of the signal-to-noise transferring properties of the X-ray detector [3,4]. The latter incorporates adequate subject image phantoms with embedded detectable structures [5,6]. The number and type of the structures detected, by an expert viewer, characterize the quality of the image. The phantoms used in the latter case may be expensive and sophisticated. In recent years 3D printing technology has evolved from exemplifying in research labs to a robust method for designing and constructing devices. Apart from the printer technology an effort has been undertaken for the synthesis of materials used for printing 3D objects. The quality of the printed objects is a function of the printing method and the printing material. Up to now in the designing and manufacturing of X-ray image phantoms 3D printing has been used for building phantoms for multimodality imaging (i.e. PET/CT and SPECT/CT) [7,8]. A cheap 3D printer however, could be used for printing a simple image phantom for a first step routine testing of 2D medical imaging, or for image quality characterization of small research detectors. The scope of this work was the use of a commercially and low cost available 3D printer for manufacturing an image quality phantom of small dimensions for 2D imaging. The build phantom was initially checked in a commercially available X-ray and detector system. Our results showed that the quality of the final object is largely affected by the material used, the printing density and the resolution capabilities of the printer.

2. Materials and Methods

2.1. Phantom concept and design

A low contrast phantom, via 123d design of AUTODESK software, was designed [9]. The phantom dimensions (width x length) were 100mm x 100mm, while the depth was 12mm. Since the state-of-the-art in low contrast measurements is the CDRAD Artinis phantom [5], our design included holes of



different depth and diameter. In more details the design included varying depth and diameter holes between 1mm up to 9mm, with step 1mm, as well as a 0.5 mm hole.

2.2. Printing conditions

A self-assembled 3D printer, geeetech i3, was used for printing the phantom. The printing material was PLA. The temperature was set at 210 °C and the material density was chosen as 100%. The printing time was 19 hours.

2.3. Irradiation conditions

The build phantom was irradiated at a Philips diagnost 93 radiological unit at high voltage settings between 40 kVp to 70 kVp with step 10 kVp. Since there was no primer for this material the semi-AEC exposure mode was chosen, that is the radiological system would set an optimum mAs value. The detector used was an Agfa cr30-x, computerized radiography system. The images obtained were assessed via ImageJ software [10]. The contrast, as the relative difference between the signal in the hole and the signal in the non-holed area of the phantom, was calculated. In addition the range of the observed depth-diameter combinations was studied by two observers inspecting the produced images.

3. Results and Discussion

In figure 1 the built phantom is shown. The weight of the phantom was 0.117 Kg. The printer capabilities did not allow the build of 0.5 mm dimension. In addition the printed diameter dimensions were measured reduced up to 0.4 mm and the printed thicknesses were measured increased up to 1.8 mm with respect to the design by AUTODESK.

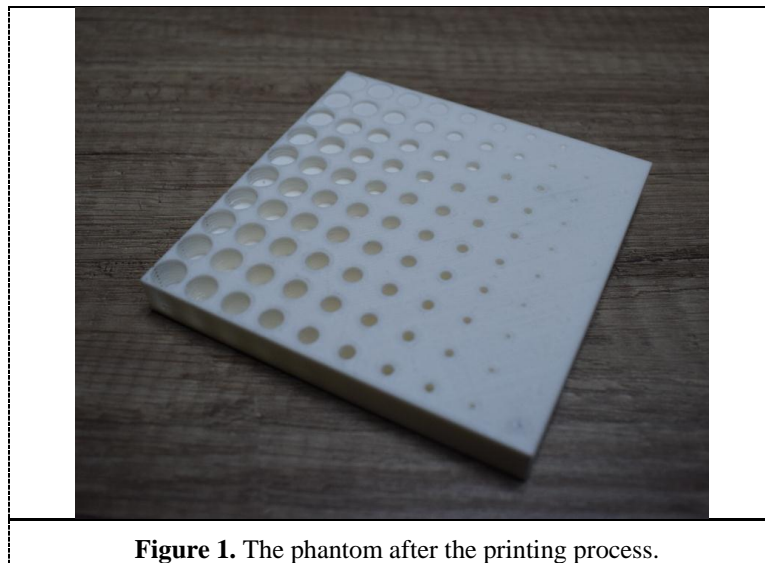


Figure 1. The phantom after the printing process.

The mAs chosen by the AEC system was 10, 8, 6.3 and 5 for 40 kVp, 50kVp, 60kVp and 70 kVp, respectively. The calculated contrast for each case was a function of the thickness of the hole, where, as expected, the hole of 9 mm depth demonstrated the highest contrast in every case. The calculated contrasts were 32.2%, 27.9%, 33.6% and 30.2% for 40 kVp, 50kVp, 60kVp and 70 kVp respectively. The contrast as a function of hole thickness, for 60 kVp is shown in figure 2.

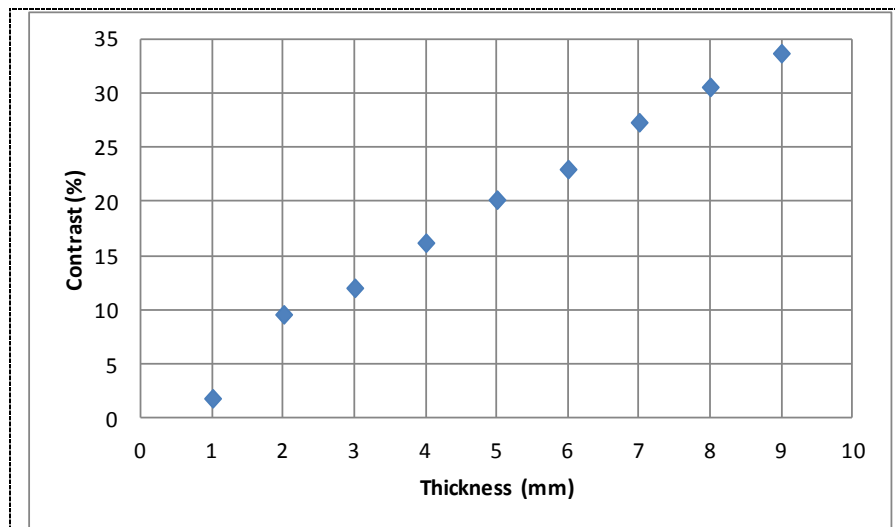


Figure 2. Contrast (%) for the 60 kVp irradiation conditions, at the 9 mm diameter holes.

The shape of figure 2 is expected since an increase in depth changes the relative X-ray transmittance in the phantom, thus the relative subject contrast. The high contrast values calculated for the 4 different kVp settings are not anticipated since the lower X-ray energies of 40 kVp are more likely to produce the highest contrast values, due to the increased photoelectric effect. In each case however a contrast around 30% is observed. A reason for this might be the software settings of Agfa cr30-x.

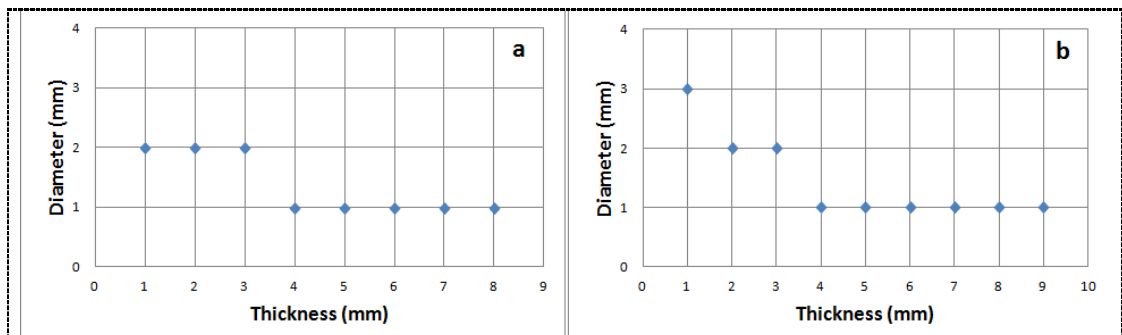


Figure 3. Hole detectability at (a) 40 kVp and (b) 70 kVp.

In figure 3 the low contrast detectability for the phantom built, under (a) 40 kVp, 10 mAs and (b) 70 kVp 5 mAs exposure conditions (semi AEC) is demonstrated. It may be seen that the 2 mm diameter and 1 mm thickness hole is distinguishable at 40 kVp, while at 70 kVp the smallest diameter visible at 1 mm depth is the 3 mm, with both observers agreeing. The information shown in figure 3 is not only a function of the observer’s performance, X-ray physics and exposure, but affected by the performance of the entire imaging chain as well. That is: (a) accuracy of kVp, (b) X-ray output reproducibility, (c) AEC and detection performance and (c) imaging software settings. Therefore the use of any low contrast detail phantom can routinely used for a first inspection of the image chain. In our case specifically the images examined by the built phantom could provide such information. However care should be taken into the printer accuracy, which yielded a reduction of the holes

dimension up to 0.4 mm. In addition the printing method yielded a printer pattern of lines in the final image, which hardened the detectability assessment of the images.

4. Conclusion

A low contrast phantom was designed and built in terms of a self assembled 3D printer. The phantom was tried out as an initial and easy approach for determining contrast and low contrast detectability image features of a Philips diagnost 93 radiological unit and an Agfa cr30-x combination. It was found that the phantom was efficient in examining contrast, but the extent of its accuracy and usage is a function of the 3D printer performance and capabilities. The phantom could be further utilized in assessing imaging capabilities of small dimensions X-ray detectors. In addition the constant printed pattern over-imposing the final image could be removed prior to image evaluation by means of bandwidth stop digital filters.

5. References

- [1] Kandarakis I S 2016 Luminescence in Medical Image Science *J. Lumin.* **169** 553.
- [2] Liaskos M, Michail C, Kalyvas N, Toutountzis A, Tsantis S, Fountos G, Cavouras D and Kandarakis I 2010 Implementation of a Software Phantom for the Assessment of Contrast Detail in Digital Radiography *e-Journal of Science & Technology* **5(2)** 15.
- [3] Michail C, Valais I, Martini N, Koukou V, Kalyvas N, Bakas A, Kandarakis I and Fountos G 2016 Determination of the Detective Quantum Efficiency (DQE) of CMOS/CsI Imaging Detectors following the novel IEC 62220-1-1:2015 International Standard *Radiat. Meas.* **94** 8.
- [4] Karpetas G E, Michail C M, Fountos G P, Kalyvas N I, Valais I G, Kandarakis I S and Panayiotakis G S 2017 Detective Quantum Efficiency (DQE) in PET Scanners: A Simulation Study *Appl. Radiat. Isot.* **125** 154.
- [5] <http://www.artinis.com/cdrad/> (last accessed August 2017).
- [6] Koukou V, Martini N, Fountos G, Michail C, Sotiropoulou P, Bakas A, Kalyvas N, Kandarakis I, Speller R, Nikiforidis G 2017 Dual energy subtraction method for breast calcification imaging *Nucl. Instrum. Meth. Phys. Res. A.* **848**, 31.
- [7] Miller B W, Moore J W, Barret H H, Frye T, Adler S, Sery J, Furenlid L R 2012 3D printing in X-ray and Gamma-Ray Imaging: A novel method for fabricating high-density imaging apertures. *Nucl. Instrum. Meth. Phys. Res. A.* **659** 262.
- [8] Bieniosel M F, Lee B J, Levin C S 2015 Characterization of custom 3D printed multimodality imaging phantoms *Med. Phys.* **42** 5913.
- [9] <https://www.autodesk.com/solutions/3d-modeling-software> (last accessed August 2017).
- [10] <https://imagej.nih.gov/ij/> (last accessed August 2017).